Unimolecular decay of Criegee intermediates to OH radical products: Prompt and thermal decay processes

Marsha I. Lester^{a*} and Stephen J. Klippenstein^b
^aDepartment of Chemistry, University of Pennsylvania, Philadelphia, PA 19104-6323
^bChemical Sciences and Engineering Division, Argonne National Laboratory, Argonne, IL 60439

Conspectus

Alkene ozonolysis is a primary oxidation pathway for anthropogenic and biogenic alkenes emitted into the troposphere. It is also an important source of atmospheric hydroxyl (OH) radicals, often called the atmosphere's detergent. Alkene ozonolysis takes place through a highly exothermic reaction pathway with multiple intermediates and barriers prior to releasing the OH radical products. This Account focuses on a key reaction intermediate with a carbonyl oxide functional group (-COO), known as the Criegee intermediate, which is formed along with a carbonyl co-product in alkene ozonolysis reactions. Under atmospheric conditions, the initally energized Criegee intermediates may promptly decay to OH products or be collisionally stabilized prior to thermal decay to OH radicals and other products. Alternatively, the stabilized Criegee intermediates may undergo bimolecular reactions with atmospheric species, including water vapor and sulfur dioxide, which can lead to nucleation and growth of aerosols.

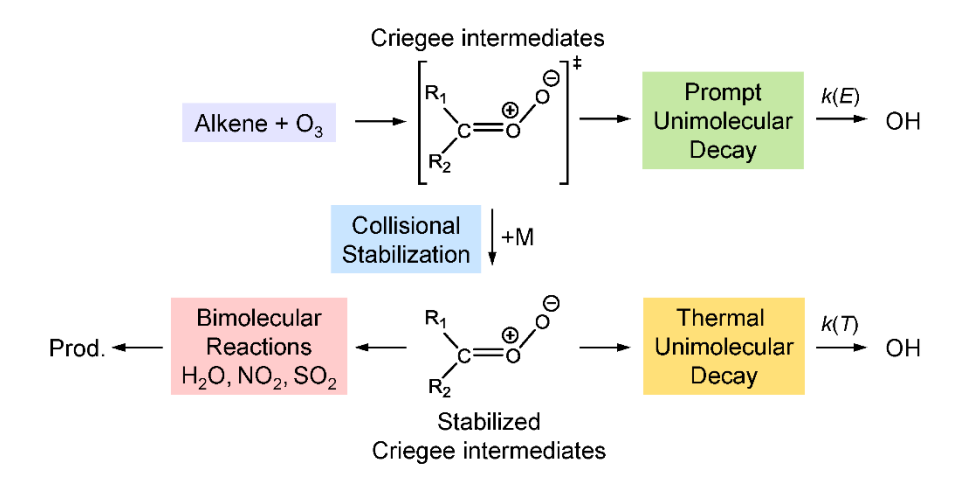
The dimethyl-substituted Criegee intermediate, (CH₃)₂COO, is utilized in this Account to showcase recent efforts to experimentally measure and theoretically predict the rates for prompt and thermal unimolecular decay processes of prototypical Criegee intermediates under laboratory and atmospheric conditions. The experimental laboratory studies utilize an alternative synthesis method to efficiently generate Criegee intermediates via the reaction of iodoalkyl radicals with O₂. Infrared excitation is then used to prepare the (CH₃)₂COO Criegee intermediates at specific energies in the vicinity of the transition state barrier or significantly below the barrier for 1,4 hydrogen transfer that leads to OH products. The rate of unimolecular decay is revealed through direct time-domain measurements of the appearance of OH products utilizing ultraviolet laser-induced fluorescence detection under collision-free conditions. Complementary high-level theoretical calculations are carried out to evaluate the transition state barrier and the energy-dependent unimolecular decay rates for (CH₃)₂COO using Rice-Ramsperger-Kassel-Marcus (RRKM) theory, which are in excellent accord with the experimental measurements. Quantum mechanical tunneling through the barrier, incorporated through Eckart and semi-classical transition state theory models, is shown to make a significant contribution to the unimolecular decay rates at energies in the vicinity of and much below the barrier. Master equation modeling is used to extend the energy-dependent unimolecular rates to thermal decay rates of (CH₃)₂COO under tropospheric conditions (high pressure limit), which agree well with recent laboratory measurements [Smith et al., J. Phys.

1

-

^{*} To whom correspondence should be addressed: milester@sas.upenn.edu

Chem. A **2016**, 120, 4789 and Chhantyal-Pun et al., *J. Phys. Chem. A* **2017**, 121, 4-15]. Again, tunneling is shown to enhance the thermal decay rate by orders of magnitude. The experimentally-validated unimolecular rates are also utilized in modeling the prompt and thermal unimolecular decay of chemically activated (CH₃)₂COO formed upon ozonolysis of 2,3-dimethyl-2-butene under atmospheric conditions [Drozd et al., *J. Phys. Chem. A* **2017**, 121, 6036-6045]. Future challenges lie in extension of these spectroscopic and dynamical methods to Criegee intermediates derived from more complex ozonolysis reactions involving biogenic alkenes.



Introduction

Criegee intermediates are carbonyl oxide (R₁R₂COO) species generated in the atmosphere through ozonolysis of alkenes originating from biogenic or anthropogenic sources.¹ Alkene ozonolysis is a major pathway for removal of volatile alkenes, organic compounds with the largest emissions into the atmosphere after methane.²⁻³ Alkene ozonolysis is also an important source of hydroxyl radicals (OH), a key oxidant that initiates the breakdown of most pollutants in the lower atmosphere. These highly exothermic ozonolysis reactions produce energized Criegee intermediates, some of which promptly decay to OH radicals.⁴⁻⁵ The remaining Criegee intermediates are collisionally stabilized and thermalized prior to decaying to OH radicals and other products.⁵⁻⁶ Alternatively, the stabilized Criegee intermediates undergo bimolecular reactions with atmospheric species, including water vapor, SO₂, NO₂, and acids,⁷⁻¹¹ which may result in aerosol formation and impact on climate.¹²

The UK Torch field campaign near London in the summer of 2003 showed that alkene ozonolysis is responsible for about a third of the atmospheric OH radicals in the daytime and essentially all of the OH radicals at nighttime. The PUMA field campaign near the urban city centre of Birmingham, UK in 1999-2000 indicated that alkene ozonolysis accounts for nearly half of the OH radicals in summertime and most of the OH radicals in the wintertime. Laboratory studies have indicated that the OH yield from ozonolysis of internal alkenes, with corresponding alkyl-substituted Criegee intermediates, is significantly greater than that from ethene ($\leq 20\%$). For example, the reported yield of OH radicals is 90% from ozonolysis of 2,3-dimethyl-2-butene, of often known as tetramethylethylene (TME), which proceeds though the dimethyl-substituted Criegee intermediate (CH₃)₂COO. Moreover, (CH₃)₂COO can be generated upon ozonolysis of any alkene with a (CH₃)₂C= functional group, including many terpenes such as mycrene and terpinolene, and thus may be significant in the atmosphere.

This Account provides an overview of recent experimental, theoretical, and master equation modeling studies of the unimolecular decay dynamics of the dimethyl-substituted Criegee intermediate $(CH_3)_2COO$ to OH radical products. This report focuses on experimental and computed microcanonical rates k(E) for unimolecular decay of $(CH_3)_2COO$ at specific energies E in the vicinity of the transition state (TS) barrier and at well-defined energies significantly below the TS barrier, which involve quantum mechanical tunneling through the barrier. Master equation modeling is used to extend the results to thermal decay rates k(T) of stabilized Criegee intermediates at temperatures T relevant to the troposphere (high pressure limit), and comparison is made to recent thermal rate measurements under laboratory flow cell conditions. Finally, the experimentally validated microcanonical rates are utilized to model the prompt and thermal unimolecular decay processes for $(CH_3)_2COO$ to OH products, starting from the chemically activated energy distribution for $(CH_3)_2COO$ anticipated upon ozonolysis of TME.

Infrared action spectra of Criegee intermediates

This laboratory has carried out fundamental studies of the infrared action spectra and unimolecular decay dynamics of the dimethyl-substituted Criegee intermediate (CH₃)₂COO to OH radical products, $^{19-20, 24-25}$ along with analogous studies of *syn* methyl- and ethyl-substituted Criegee intermediates. $^{19, 26-30}$ Our laboratory uses an alternative synthesis method $^{31-32}$ to

efficiently produce the Criegee intermediates via the reaction of iodoalkyl radicals, photolytically generated from diiodo alkane precursors, with O_2 in a quartz capillary reactor tube prior to free jet expansion. We have demonstrated that vibrational activation of cold alkyl-substituted Criegee intermediates can be utilized to drive hydrogen transfer from an α -H on the *syn*-methyl (or ethyl) group to the terminal oxygen atom, which is followed by rapid dissociation to OH radical products. $^{25, 28, 30}$

As illustrated in Figure 1, IR excitation of $(CH_3)_2COO$ with two quanta of CH stretch $(2v_{CH})$ or one quantum each of CH stretch and another lower frequency mode $(v_{CH}+v_i)$ is combined with sensitive UV laser-induced fluorescence (LIF) detection of the OH $X^2\Pi$ (v=0) products to reveal the infrared action spectra of the Criegee intermediates under collision-free conditions. Unimolecular decay proceeds by 1,4-hydrogen transfer via a five-membered, ring-like transition state (TS) to form a methyl-substituted vinyl hydroperoxide (VHP, $H_2C=C(CH_3)OOH$) species. This rate-limiting 1,4 H-atom transfer step to VHP is followed by rapid homolysis of the O-O bond to form OH + methyl-substituted vinoxy ($H_2C=C(CH_3)O$) products. An analogous pathway occurs for the more stable syn-conformers of CH_3CHOO and CH_3CH_2CHOO . A different reaction pathway is predicted for the simplest Criegee intermediate CH_2OO , for which unimolecular decay involves a much higher barrier to initially form dioxirane, 5 consistent with the lower OH yield and other products observed in corresponding ozonolysis reactions. The anti-conformer of CH_3CHOO is also predicted to decay via isomerization to methyldioxirane, which leads to many products including OH radicals.

The IR action spectra of (CH₃)₂COO shown in Figure 2 are obtained by scanning the tunable IR radiation from a KTP-based optical parametric oscillator/amplifier to access CH overtone transitions ($2v_{CH}$) in the 5600-6000 cm⁻¹ region at a fixed IR-UV time delay of 67 ns and combination bands ($v_{CH}+v_i$) in the 3950-4500 cm⁻¹ region with a time delay of 1.5 μ s. ^{19-20, 25} The resultant IR action spectra reveal vibrational states with significant IR oscillator strength at these energies, as evident by the excellent agreement with the computed IR spectra of (CH₃)₂COO. ^{19-20, 25} The vibrational excitation must also supply sufficient energy to surmount or tunnel through the barrier for unimolecular rearrangement and dissociation to OH products, which are detected by LIF. A few of the features exhibit distinctive rotational band contours and display homogeneous broadening attributed to rapid (ps) energy randomization, known as intramolecular vibrational energy redistribution (IVR), following IR excitation. Most remarkably, many (CH₃)₂COO spectral features are observed at energies considerably below the theoretically predicted TS barrier height of 16.16 kcal mol⁻¹ (5651 cm⁻¹), which is derived from high-level electronic structure calculations with zero-point energy (ZPE) and other corrections.¹⁹ This was the first suggestion of significant quantum mechanical tunneling of the transferring Hatom through the TS barrier, 25 which was later validated through experimental and theoretical studies of the rates for unimolecular decay. 19-20

Unimolecular decay dynamics of Criegee intermediates

We have also made direct time-domain measurements of the rate of appearance of OH products following vibrational activation of $(CH_3)_2COO$, and other prototypical alkylsubstituted Criegee intermediates under collision-free conditions. In Infrared excitation of distinct features of $(CH_3)_2COO$ in the 5600-6000 cm⁻¹ region is used to prepare the Criegee

intermediates at specific energies in the vicinity of the TS barrier (5651 cm⁻¹). ¹⁹ Similarly, vibrational activation of different transitions of (CH₃)₂COO in the 3950-4500 cm⁻¹ region prepares the Criegee intermediates at discrete energies significantly below the TS barrier.²⁰ In both energy regimes, the rate of appearance of OH products is measured by varying the IR-UV time delay with UV LIF detection of OH products. Representative OH temporal profiles are shown in Figure 3 following IR activation of (CH₃)₂COO at 5971.0 cm⁻¹ and 4295.6 cm⁻¹ with OH appearance times (and corresponding rates) of 18.5 \pm 1.0 ns (5.4 \pm 0.3 x 10⁷ s⁻¹) and 1650 \pm 220 ns $(6.1 \pm 0.8 \times 10^5 \text{ s}^{-1})$, respectively. The significantly different risetimes are taken into account in the fixed IR-UV delays utilized for IR action spectra (Figure 2). The exponential fall off is attributed to molecules moving out of the spatial region irradiated by the UV probe laser. It is separately determined at long IR-UV delay times where the exponential fall off dominates (≥ 95% contribution). The rate of appearance of OH products depends sensitively on the excitation energy as shown in Figures 3 and 4. The appearance of OH products occurs on a tens of nanosecond timescale in the vicinity of the TS barrier, corresponding to rates of ca. 10⁷ s⁻¹. By contrast, the OH products appear on a 100-fold slower timescale at energies as much as 1500 cm⁻¹ below the TS barrier, corresponding to rates of ca. 10⁵ s⁻¹.

For comparison, we carried out statistical RRKM calculations of the microcanonical dissociation rates for (CH₃)₂COO over a wide range of energies¹⁹⁻²⁰

$$k(E) = \frac{\sigma_{eff}}{\sigma_{eff}} \frac{G^{\dagger}(E - E_0)}{hN(E)}$$

Here, E_0 is energy of the transition state (TS) barrier, $G^{\dagger}(E-E_0)$ is the sum of states at the TS, N(E) is the density of states of the $(CH_3)_2COO$ reactant, and h is Planck's constant. The effective symmetry numbers σ_{eff} are 1 for the reactant and 1/2 for the transition state. Details of the high-level electronic structure and anharmonic vibrational frequency calculations are presented elsewhere. Two different tunneling models are implemented for the 1,4 H-atom transfer step, Eckart and semiclassical transition state theory (SCTST), with an imaginary frequency of 1572 i cm⁻¹ as described in previous work.

Quite remarkably, the unimolecular dissociation rates computed for (CH₃)₂COO using statistical RRKM theory with tunneling (Eckart and SCTST) are in nearly quantitative agreement with the experimental rates of appearance of OH products in the 5600-6000 cm⁻¹ region as shown in Figure 4. The exquisite agreement of experiment and a priori theory validates the computed TS barrier height¹⁹ and tunneling rates, and also confirms that the initial vibrational excitation is randomized prior to unimolecular decay. Notably, due to the presence of significant multi-reference character in the wavefunction for Criegee intermediates, the accurate prediction of the barrier height relies on the inclusion of higher-order corrections to the gold-standard CCSD(T) coupled cluster method. These corrections were evaluated with the CCSDT(Q) method, which incorporates corrections for triple and quadruple electron excitations. In the 3950-4500 cm⁻¹ region, the Eckart model predicted rates that are a little faster than experiment.²⁰ As a result, the Eckart parameters were adjusted slightly (5% decrease in imaginary frequency and <1% decrease in TS barrer, both of which are well within the expected accuracy of the calculations), which gave excellent agreement with the experimental data in

both energy regions. The calculations also showed that the 100-fold decrease in the unimolecular decay rate at energies substantially below the TS barrier is primarily due to the reduced tunneling probability in the H-atom transfer step. Without including tunneling in the RRKM calculations, the predicted rates are dramatically different than experiment with slower unimolecular rates above and no reaction below the TS barrier as shown in Figure 4.

Thermal decay of Criegee intermediates

Master equation modeling has been used to extend the experimental and/or computed microcanonical decay rates k(E) to thermal decay rates k(T) of stabilized Criegee intermediates from alkene ozonolysis in the troposphere (high pressure limit). 19-20, 28-29 The thermal decay rates are effectively a Boltzmann weighted average of the microcanonical rates over a range of energies E^{37}

$$k(T) \propto \int k(E)N(E) \exp(-E/k_BT)dE$$

Here, N(E) is the density of states of the $(CH_3)_2COO$ reactant and $exp(-E/k_BT)$ is an exponential Boltzmann factor representing the population distribution of the collisionally stabilized Criegee intermediates at a temperature T. Evaluation of the integrand shows that energies of ca. 4000 cm⁻¹ in the deep tunneling regime make the largest contribution to the thermal decay rate of $(CH_3)_2COO$ at 300 K. Thus, the direct time-domain measurements in the 3950-4500 cm⁻¹ regime provide important further validation for the theory-based thermal rate predictions.

We have predicted the thermal decay rates k(T) for $(CH_3)_2COO$ at temperatures relevant in the troposphere (230-300 K) in the high pressure limit²⁰ and display the results in Figure 5. The Arrhenius plot (semi-log plot of k vs. 1000/T) exhibits strong curvature indicative of the very important role of quantum mechanical tunneling in the thermal rate. At 298 K, we predict k(T) to be 276 s⁻¹, corresponding to a decay time of ca. 3.6 ms. The thermal rates are orders of magnitude faster than those evaluated without including tunneling as shown in Figure 5. Without tunneling, the Arrhenius plot is linear with its slope determined by the TS barrier height.

Our predicted thermal rate coefficient of $276 \, s^{-1}$ at $298 \, K$ agrees well with two subsequent experimental measurements of $361 \pm 49 \, s^{-1}$ ($298 \, K$) and $305 \pm 70 \, s^{-1}$ ($293 \, K$) for the unimolecular thermal decay of $(CH_3)_2COO.^{21-22}$ A strong temperature-dependence in the thermal rate was reported from $283 \, to \, 323 \, K,^{21}$ which is in good accord with our master-equation modeling including tunneling (Figure 4).²⁰ Other recent studies, for example Newland et al.,³⁸ report a ratio of the thermal unimolecular decay rate for $(CH_3)_2COO$, derived from TME ozonolysis, relative to its bimolecular reaction rate with SO_2 . The thermal decay rates are extremely challenging to measure³⁹ because of bimolecular loss from the many reactive species present and/or wall loss over long time scales (ms). Similar master equation modeling has been performed for syn-conformers of CH_3CHOO and CH_3CH_2CHOO , again based on experimenally validated microcanonical rates, yielding thermal rates of 122 and 279 s⁻¹ at 298 K (high pressure limit), respectively.^{19, 28-29} Other purely theoretical thermal rate predictions for syn- CH_3CHOO are $124 \, s^{-1}$ and $328 \, s^{-1}$ at $298 \, K.^{40-41}$

The thermal rates can be contrasted with the recently reported rates for competing bimolecular reactions of $(CH_3)_2COO$ with water vapor (70% relative humidity, RH) and SO_2 (ca. 50 ppb) under atmospheric conditions with slower effective first-order rates of $10\text{-}100 \text{ s}^{-1}$. 22 , 42 This demonstrates that thermal unimolecular decay of $(CH_3)_2COO$ to OH products will dominate over its bimolecular reactions with water vapor and SO_2 . Vereecken et al. have computed unimolecular reaction rates for the decomposition of stabilized Criegee intermediates through a wide-range of pathways utilizing theory-based structure—activity relationships. 43 For $(CH_3)_2COO$ undergoing 1,4-H-migration, they predict a unimolecular decay rate of 478 s⁻¹ at 298 K, which is faster than our estimate or recent measurements. Current atmospheric models assume estimated rates of $100\text{-}200 \text{ s}^{-1}$ for thermal unimolecular loss of stabilized Criegee intermediates. $^{44\text{-}46}$

For the simplest Criegee intermediate CH_2OO , thermal decay is not the dominant loss process in the atmosphere. For CH_2OO , other groups have recently shown that its bimolecular reaction with water vapor, specifically the water dimer, is the dominant tropospheric loss process. The bimolecular reaction of CH_2OO with $(H_2O)_2$ at 70% RH at 298 K was found to have a very fast effective rate of 3900 s⁻¹, which is much faster than its bimolecular reactions with other atmospheric species. $^{10-11}$ C_2H_4 ozonolysis experiments have shown that the thermal decay rate for CH_2OO is very slow at 0.19 ± 0.07 s⁻¹. This is due to the higher barrier to dioxirane (~19.1 kcal mol⁻¹), which is generally thought to be followed by transformation to activated (or "hot") formic acid that fragments into OH and other products. The less stable anti-conformer of CH_3CHOO , in which the CH_3 group points away from the terminal O, also reacts quickly with water vapor. $^{32,52-53}$

Prompt and thermal decay of chemically activated Criegee intermediates

Drozd et al. have also carried out master equation modeling of the prompt and thermal decay of chemically activated (CH₃)₂COO formed upon ozonolysis of TME under atmospheric conditions (1 atm, 298 K).²³ Again, the modeling is based on our experimentally-validated microcanonical rate constants k(E) for the unimolecular decay of $(CH_3)_2COO$ to OH products (Figure 4). 19-20 The energy released in the ozonolysis reaction is assumed to be statistically partitioned between (CH₃)₂COO, the carbonyl (acetone) coproduct, and translational degrees of freedom. The internal energy of (CH₃)₂COO is also constrained to match the experimental pressure-dependent yields of stabilized Criegee intermediates (up to 0.3 at 1 atm) reported by Hakala and Donahue for TME ozonolysis at 298 K.⁵⁴ The resultant chemically activated (CH₃)₂COO formed upon TME ozonolysis is estimated to have an average energy of 8500 cm⁻¹ in a Gaussian-like distribution with a breadth (FWHM) of 6000 cm⁻¹. The chemically activated Criegee intermediates will undergo collisional relaxation with bath gas (N₂ and O₂ in air at 1 atm) at a rate of ca. 10¹⁰ s⁻¹, and the average energy transferred per collision is assumed to be ca. 250 cm⁻¹. Many collisions are required for thermalization and stabilization of the Criegee intermediates, which is estimated to occur in ca. 100 ns. The slower bimolecular reactions^{22, 42} with water vapor, SO₂, or other atmospheric species are not included in the model.

Drozd et al. focused on the time evolution of OH radical products, which separates into three regimes. At early times (≤ 100 ns), the highest energy portion of the chemically activated (CH₃)₂COO distribution with energies above the TS barrier and $k(E) > 10^7$ s⁻¹ will undergo prompt

unimolecular decay to OH products. This occurs more rapidly than (CH₃)₂COO suffering more than a few collisions. At intermediate times, the remaining portion of the (CH₃)₂COO distribution will be collisionally thermalized and form stabilized Criegee intermediates. At long times, this stabilized part of the (CH₃)₂COO distribution will undergo thermal unimolecular decay that occurs on a much longer timescale (~3 ms at 298 K and 1 atm). As shown in Figure 6, more than half of the OH yield (0.63) is predicted to occur by prompt unimolecular decay within the first 100 ns. Next, there is a period of negligible OH formation, in which collisional thermalization and stabilization of (CH₃)₂COO is occurring, followed by the onset of thermal unimolecular decay at ca. 50 μs. Thermal OH production continues for ca. 30 ms, generating the remaining OH product yield (0.37). As evident in Figures 4 and 5, tunneling has a significant impact on the prompt and thermal rates. The prompt unimolecular decay rate of chemical activated (CH₃)₂COO is enhanced due to tunneling. Tunneling also increases the thermal unimolecular decay rate of (CH₃)₂COO by ca. 30x under atmospheric conditions; without tunneling, thermal OH production would occur on much slower timescale ranging from 1 ms to 1 s. Very recently, Kuwata and coworkers have done further statistical modeling of the VHP, hydroxyacetone,⁵⁵ and OH products formed upon TME and trans-2-butene ozonolysis.⁵⁶

Uncertainties in the initial energy (and angular momentum) distribution of the Criegee intermediate and in its rate of collision-induced energy relaxation are now the greatest remaining challenges to quantitatively predicting the overall branching to stabilized Criegee intermediate in the ozonolysis process. A recent study has demonstrated the utility of coupling directory trajectories with high level ab initio transition state theory based master equation modeling to predict the initial energy and angular momentum distribution arising in ethylene ozonoloysis.⁵⁷ Meanwhile, trajectory based determinations of the energy and angular momentum transfer kernel can be directly coupled with the 2-dimensional master equation to account quantitatively for the collisional relaxation process.⁵⁸

Conclusions

Recent experimental, theoretical, and master equation modeling studies of the dimethyl-substituted Criegee intermediate $(CH_3)_2COO$ and its unimolecular decay dynamics to OH radical products are reviewed. Experimental measurements of the microcanonical rates k(E) for unimolecular decay of $(CH_3)_2COO$ are obtained at specific energies E in the vicinity of the transition state (TS) barrier and at well-defined energies significantly below the TS barrier, and are shown to be in excellent agreement with RRKM calculations that include quantum mechanical tunneling through the barrier. Master equation modeling is used to extend the results to thermal decay rates k(T) of stabilized Criegee intermediates under tropospheric conditions (high pressure limit), again showing the important role of tunneling. Finally, the experimentally validated microcanonical rates have been incorporated in a model of the unimolecular decay processes for a chemically activated energy distribution of $(CH_3)_2COO$ under atmospheric conditions. The challenge for the future is to extend the spectroscopic and dynamical studies of Criegee intermediates to those derived from ozonolysis of biogenic alkenes. Additional unimolecular decay pathways and reaction products are predicted to be important based on structure—activity relationships. The challenge for the future is to extend the spectroscopic alkenes.

Acknowledgements

This work was primarily supported by National Science Foundation Grants CHE-1362835 and CHE-1664572 (to M.I.L.). This material is also based on work supported by the US Department of Energy, Office of Science, Office of Basic Energy Sciences, Division of Chemical Sciences, Geosciences, and Biosciences at Argonne under Contract DE-AC02-06CH11357 (to S.J.K.). This Account is an overview of the outstanding research conducted by many talented graduate students and postdoctoral scholars, including Fang Liu, Joseph M. Beames, Andrew S. Petit, Yi Fang, Victorial P. Barber, Greg Drozd, Nathanael M. Kidwell, Hongwei Li, and Amy M. Green. M.I.L. also thanks senior collaborators Anne B. McCoy (University of Washington) and Neil Donahue (Carnegie Mellon University).

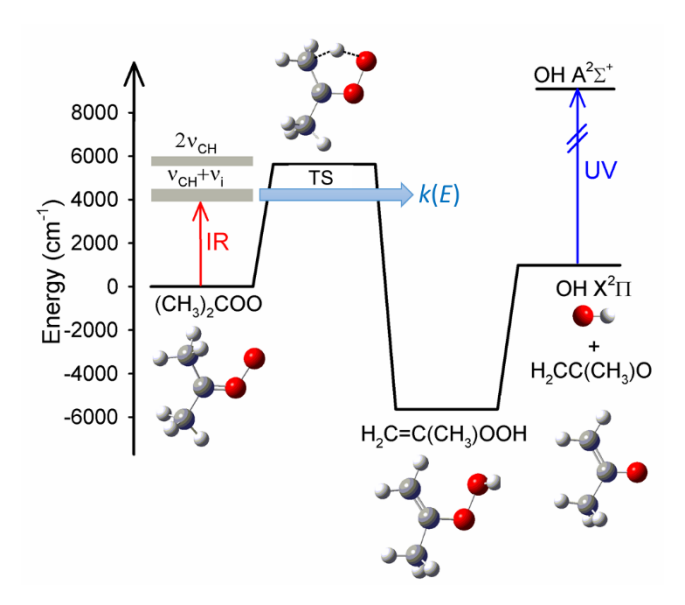


Figure 1. Reaction coordinate predicted from the $(CH_3)_2COO$ Criegee intermediate to OH products. The reaction follows a rate-limiting 1,4-hydrogen transfer to a methyl-substituted vinyl hydroperoxide (VHP, $CH_2=C(CH_3)OOH$) species via a transition state (TS), followed by rapid decomposition to OH + methyl-substituted vinoxy ($H_2C=C(CH_3)O$) products. In laboratory studies, the IR laser prepares the Criegee intermediates with two quanta of CH stretch ($2v_{CH}$) or CH stretch and a lower frequency mode ($v_{CH}+v_i$), while the OH products are state-selectively detected by UV laser-induced fluorescence (LIF). The rate of appearance of OH products is measured by varying the time delay between the IR and UV laser pulses. Adapted with permission from ref. 19. 2016 AIP Publishing.

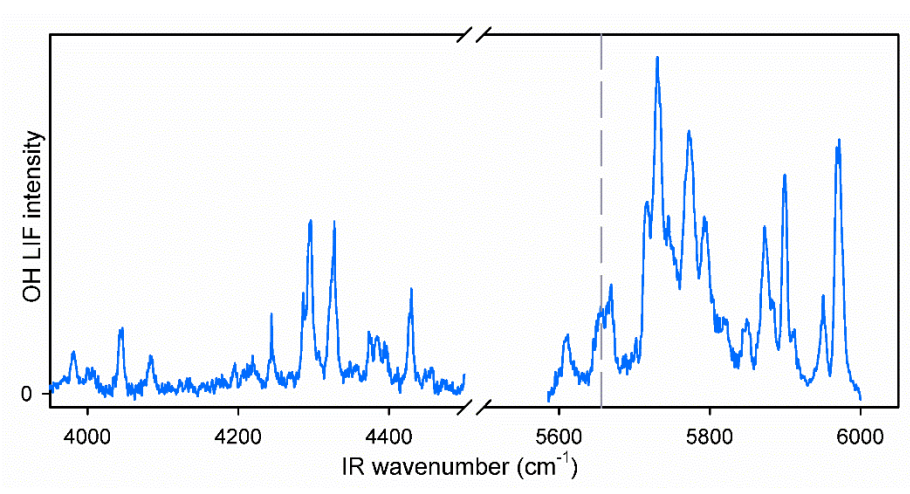


Figure 2. Compilation of experimental IR action spectra of $(CH_3)_2COO$ Criegee intermediates with UV laser-induced fluorescence (LIF) detection of OH products. The $(CH_3)_2COO$ spectral features in the 3950-4500 cm⁻¹ region arise from excitation of CH stretch and a lower frequency mode $(v_{CH}+v_i)$, while those in the 5600-6000 cm⁻¹ region involve two quanta of CH stretch $(2v_{CH})$ excitation. These IR transitions enable excitation of $(CH_3)_2COO$ at energies near and significantly below the TS barrier (dashed vertical gray line). The 3950-4500 and 5600-6000 cm⁻¹ regions were recorded at IR-UV time delays of 1.5 μ s and 67 ns, respectively. The relative intensities in the two spectral regions were scaled to match the computed IR intensities for the strongest transition in each region. Adapted with permission from ref. 19. 2016; ref. 20. 2017; and ref. 25. 2014 AIP Publishing.

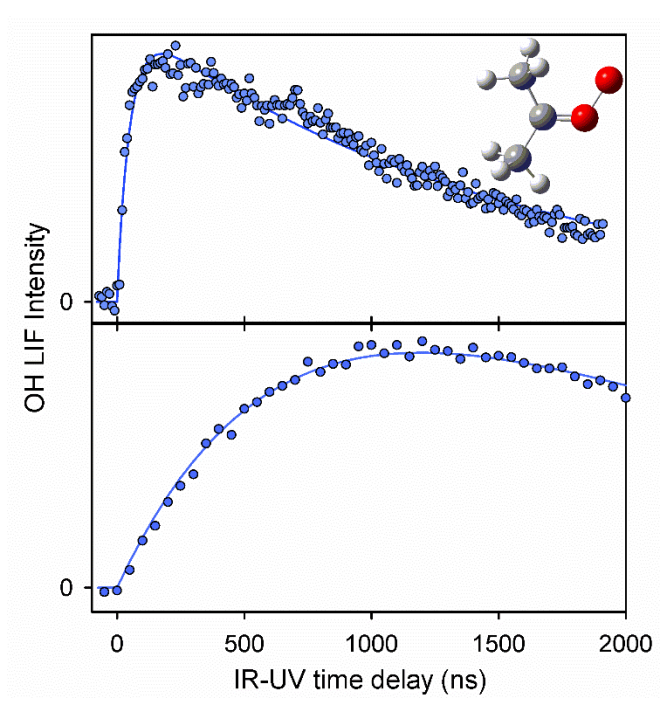


Figure 3. Representative temporal profiles of OH products following IR activation of $(CH_3)_2COO$ at 5971.0 cm⁻¹ (top panel) and 4295.6 cm⁻¹ (bottom panel) recorded as a function of IR-UV time delay. The exponential rise is due to unimolecular decay of $(CH_3)_2COO$, while the exponential fall off is attributed to molecules moving out of the spatial region irradiated by the UV probe laser. The appearance of OH products decreases by ca. 100 fold at energies significantly below the TS barrier. Adapted with permission from ref. 19. 2016 and ref. 20. 2017 AIP Publishing.

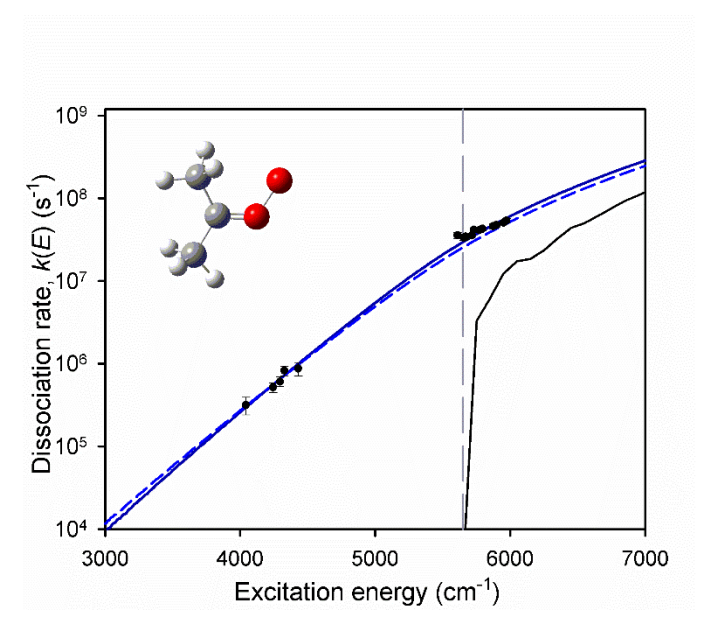


Figure 4. Experimental and computed microcanonical dissociation rates k(E) (semi-log scale) for the $(CH_3)_2COO$ Criegee intermediate to OH radical products in the energy E range from 3000 to 7000 cm⁻¹. Experimental rates (black symbols with error bars) are obtained from the temporal profiles of OH products following IR activation of $(CH_3)_2COO$ at energies near and significantly below the TS barrier (dashed vertical gray line). Statistical RRKM rates k(E) are computed using adjusted Eckart (dark blue line) and semi-classical transition state theory (SCTST, dashed blue line) models for tunneling. The importance of tunneling through the TS barrier is illustrated by the RRKM rates computed without tunneling (black line). Adapted with permission from ref. 20. 2017 AIP Publishing.

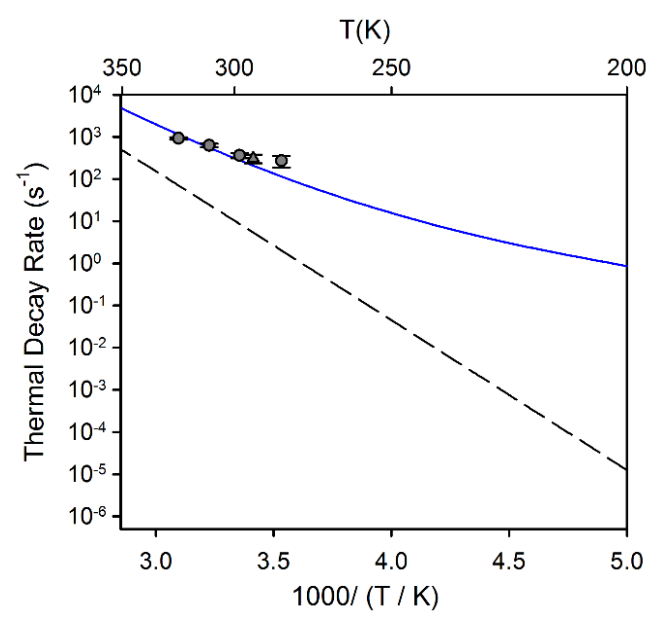


Figure 5. Arrhenius plot of thermal decay rate k(T) predicted from master equation modeling of the unimolecular decay of $(CH_3)_2COO$ to OH products (high-pressure limit) over temperature range from 200 to 350 K (blue). Tunneling increases the thermal rate by orders of magnitude as illustrated by analogous calculations neglecting tunneling (dashed gray line). Also shown are recent thermal decay rate measurements for $(CH_3)_2COO.^{21,22}$

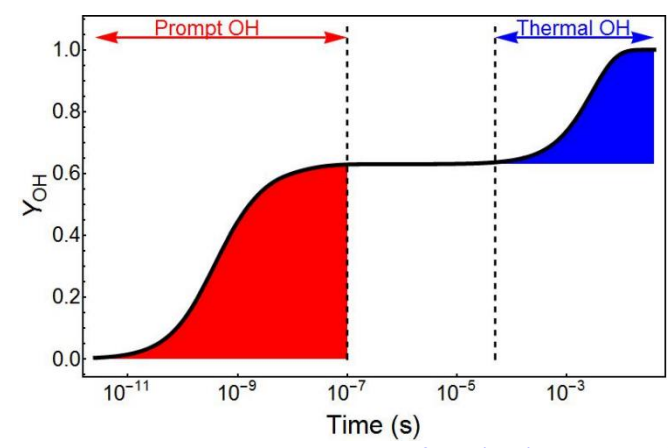


Figure 6. Time-dependent yield of OH (Y_{OH}) predicted for TME ozonolysis under atmospheric conditions (1 atm, 298 K).²³ Prompt OH production (red) occurs within 100 ns of Criegee intermediate formation, followed by negligible OH formation until the onset of thermal decay (blue) at 50 μ s.

Biographical Information

Stephen J. Klippenstein is a Distinguished Fellow at Argonne National Laboratory, where he works on developing and applying theoretical methods for studying the kinetics and dynamics of gas phase chemical reactions. He received his B.Sc. from University of British Columbia and Ph.D. from Caltech. Following postdoctoral research at University of Colorado, Boulder, he was a faculty member at Case Western Reserve University. He moved to Argonne in 2005 after 5 years at the Combustion Research Facility in Sandia National Laboratories, Livermore. Marsha I. Lester is the Edmund J. Kahn Distinguished Professor in the Department of Chemistry at the University of Pennsylvania, where she employs novel spectroscopic and dynamical methods to rigorously characterize reaction intermediates of environmental relevance. Her academic training included a B.A. from Douglass College, Rutgers University, Ph.D. from Columbia University, and postdoctoral research at Bell Laboratories.

References

- 1. Johnson, D.; Marston, G., The gas-phase ozonolysis of unsaturated volatile organic compounds in the troposphere. *Chem. Soc. Rev.* **2008**, *37*, 699-716.
- 2. Goldstein, A. H.; Galbally, I. E., Known and unexplored organic constituents in the Earth's atmosphere. *Environ. Sci. Technol.* **2007**, *41*, 1514-1521.
- 3. Nriagu, J. O., *Gaseous Pollutants: Characterization and Cycling*. John Wiley & Sons, Inc: New York, 1992; Vol. 24.
- 4. Alam, M. S.; Camredon, M.; Rickard, A. R.; Carr, T.; Wyche, K. P.; Hornsby, K. E.; Monks, P. S.; Bloss, W. J., Total radical yields from tropospheric ethene ozonolysis. *Phys. Chem. Chem. Phys.* **2011**, *13*, 11002-11015.
- 5. Donahue, N. M.; Drozd, G. T.; Epstein, S. A.; Presto, A. A.; Kroll, J. H., Adventures in ozoneland: Down the rabbit-hole. *Phys. Chem. Chem. Phys.* **2011**, *13*, 10848-10857.
- 6. Novelli, A.; Vereecken, L.; Lelieveld, J.; Harder, H., Direct observation of OH formation from stabilised Criegee intermediates. *Phys. Chem. Chem. Phys.* **2014**, *16*, 19941-19951.
- 7. Mauldin III, R. L.; Berndt, T.; Sipila, M.; Paasonen, P.; Petaja, T.; Kim, S.; Kurten, T.; Stratmann, F.; Kerminen, V. M.; Kulmala, M., A new atmospherically relevant oxidant of sulphur dioxide. *Nature* **2012**, *488*, 193-196.
- 8. Osborn, D. L.; Taatjes, C. A., The physical chemistry of Criegee intermediates in the gas phase. *Int. Rev. Phys. Chem.* **2015**, *34*, 309-360.
- 9. Lee, Y.-P., Perspective: Spectroscopy and kinetics of small gaseous Criegee intermediates. *J. Chem. Phys.* **2015**, *143*, 020901.
- 10. Taatjes, C. A., Criegee intermediates: What direct production and detection can teach us about reactions of carbonyl oxides. *Annu. Rev. Phys. Chem.* **2017**, *68*, 183-207.
- 11. Jr-Min Lin, J.; Chao, W., Structure-dependent reactivity of Criegee intermediates studied with spectroscopic methods. *Chem. Soc. Rev.* **2017**, *46*, 7483-7497.
- 12. Mentel, T. F.; Springer, M.; Ehn, M.; Kleist, E.; Pullinen, I.; Kurtén, T.; Rissanen, M.; Wahner, A.; Wildt, J., Formation of highly oxidized multifunctional compounds: Autoxidation of peroxy radicals formed in the ozonolysis of alkenes deduced from structure–product relationships. *Atmos. Chem. Phys.* **2015**, *15*, 6745-6765.
- 13. Emmerson, K. M.; Carslaw, N.; Carslaw, D. C.; Lee, J. D.; McFiggans, G.; Bloss, W. J.; Gravestock, T.; Heard, D. E.; Hopkins, J.; Ingham, T.; Pilling, M. J.; Smith, S. C.; Jacob, M.; Monks, P. S., Free radical modelling studies during the UK TORCH Campaign in Summer 2003. *Atmos. Chem. Phys.* **2007**, *7*, 167-181.
- 14. Emmerson, K. M.; Carslaw, N., Night-time radical chemistry during the TORCH campaign. *Atmos. Environ.* **2009**, *43*, 3220-3226.
- 15. Harrison, R. M.; Yin, J.; Tilling, R. M.; Cai, X.; Seakins, P. W.; Hopkins, J. R.; Lansley, D. L.; Lewis, A. C.; Hunter, M. C.; Heard, D. E.; Carpenter, L. J.; Creasey, D. J.; Lee, J. D.; Pilling, M. J.; Carslaw, N.; Emmerson, K. M.; Redington, A.; Derwent, R. G.; Ryall, D.; Mills, G.; Penkett, S. A., Measurement and modelling of air pollution and atmospheric chemistry in the U.K. West Midlands conurbation: Overview of the PUMA Consortium project. *Sci. Total Environ.* **2006**, *360*, 5-25.
- 16. Paulson, S. E.; Orlando, J. J., The reactions of ozone with alkenes: An important source of HOx in the boundary layer. *Geophys. Res. Lett.* **1996,** *23*, 3727-3730.
- 17. Orzechowska, G. E.; Paulson, S. E., Production of OH radicals from the reactions of C₄-C₆ internal alkenes and styrenes with ozone in the gas phase. *Atmos. Environ.* **2002**, *36*, 571-581.
- 18. Fenske, J. D.; Hasson, A. S.; Paulson, S. E.; Kuwata, K. T.; Ho, A.; Houk, K. N., The pressure dependence of the OH radical yield from ozone-alkene reactions. *J. Phys. Chem. A* **2000**, *104*, 7821-7833.

- 19. Fang, Y.; Liu, F.; Barber, V. P.; Klippenstein, S. J.; McCoy, A. B.; Lester, M. I., Communication: Real time observation of unimolecular decay of Criegee intermediates to OH radical products. *J. Chem. Phys.* **2016**, *144*, 061102.
- 20. Fang, Y.; Barber, V. P.; Klippenstein, S. J.; McCoy, A. B.; Lester, M. I., Tunneling effects in the unimolecular decay of (CH₃)₂COO Criegee intermediates to OH radical products. *J. Chem. Phys.* **2017**, *146*, 134307.
- 21. Smith, M. C.; Chao, W.; Takahashi, K.; Boering, K. A.; Lin, J. J.-M., Unimolecular decomposition rate of the Criegee intermediate (CH₃)₂COO measured directly with UV absorption spectroscopy. *J. Phys. Chem. A* **2016**, *120*, 4789-4798.
- 22. Chhantyal-Pun, R.; Welz, O.; Savee, J. D.; Eskola, A. J.; Lee, E. P. F.; Blacker, L.; Hill, H. R.; Ashcroft, M.; Khan, M. A. H.; Lloyd-Jones, G. C.; Evans, L.; Rotavera, B.; Huang, H.; Osborn, D. L.; Mok, D. K. W.; Dyke, J. M.; Shallcross, D. E.; Percival, C. J.; Orr-Ewing, A. J.; Taatjes, C. A., Direct measurements of unimolecular and bimolecular reaction kinetics of the Criegee intermediate (CH₃)₂COO. *J. Phys. Chem. A* **2017**, *121*, 4-15.
- 23. Drozd, G. T.; Kurtén, T.; Donahue, N. M.; Lester, M. I., Unimolecular decay of the dimethyl-substituted criegee intermediate in alkene ozonolysis: Decay time scales and the importance of tunneling. *J. Phys. Chem. A* **2017**, *121*, 6036-6045.
- 24. Li, H.; Kidwell, N. M.; Wang, X.; Bowman, J. M.; Lester, M. I., Velocity map imaging of OH radical products from IR activated (CH₃)₂COO Criegee intermediates. *J. Chem. Phys.* **2016**, *145*, 104307.
- 25. Liu, F.; Beames, J. M.; Lester, M. I., Direct production of OH radicals upon CH overtone activation of (CH₃)₂COO Criegee intermediates. *J. Chem. Phys.* **2014**, *141*, 234312.
- 26. Green, A. M.; Barber, V. P.; Fang, Y.; Klippenstein, S. J.; Lester, M. I., Selective deuteration illuminates the importance of tunneling in the unimolecular decay of Criegee intermediates to hydroxyl radical products. *Proc. Natl. Acad. Sci.* **2017**, *114*, 12372-12377.
- 27. Kidwell, N. M.; Li, H.; Wang, X.; Bowman, J. M.; Lester, M. I., Unimolecular dissociation dynamics of vibrationally activated CH₃CHOO Criegee intermediates to OH radical products. *Nat. Chem.* **2016**, *8*, 509-514.
- 28. Fang, Y.; Liu, F.; Klippenstein, S. J.; Lester, M. I., Direct observation of unimolecular decay of CH₃CH₂CHOO Criegee intermediates to OH radial products. *J. Chem. Phys.* **2016**, *145*, 044312.
- 29. Fang, Y.; Liu, F.; Barber, V. P.; Klippenstein, S. J.; McCoy, A. B.; Lester, M. I., Deep tunneling in the unimolecular decay of CH₃CHOO Criegee intermediates to OH radical products. *J. Chem. Phys.* **2016**, *145*, 234308.
- 30. Liu, F.; Beames, J. M.; Petit, A. S.; McCoy, A. B.; Lester, M. I., Infrared-driven unimolecular reaction of CH₃CHOO Criegee intermediates to OH radical products. *Science* **2014**, *345*, 1596-1598.
- 31. Welz, O.; Savee, J. D.; Osborn, D. L.; Vasu, S. S.; Percival, C. J.; Shallcross, D. E.; Taatjes, C. A., Direct Kinetic Measurements of Criegee Intermediate (CH₂OO) Formed by Reaction of CH₂I with O₂. *Science* **2012**, *335*, 204-207.
- 32. Taatjes, C. A.; Welz, O.; Eskola, A. J.; Savee, J. D.; Scheer, A. M.; Shallcross, D. E.; Rotavera, B.; Lee, E. P. F.; Dyke, J. M.; Mok, D. K. W.; Osborn, D. L.; Percival, C. J., Direct Measurements of conformer-dependent reactivity of the Criegee intermediate CH₃CHOO. *Science* **2013**, *340*, 177-180.
- 33. Beames, J. M.; Liu, F.; Lu, L.; Lester, M. I., Ultraviolet spectrum and photochemistry of the simplest Criegee intermediate CH₂OO. *J. Am. Chem. Soc.* **2012**, *134*, 20045-20048.
- 34. Kurten, T.; Donahue, N. M., MRCISD studies of the dissociation of vinylhydroperoxide, CH₂CHOOH: There is a saddle point. *J. Phys. Chem. A* **2012**, *116*, 6823-6830.
- 35. Nguyen, T. L.; Lee, H.; Matthews, D. A.; McCarthy, M. C.; Stanton, J. F., Stabilization of the simplest Criegee intermediate from the reaction between ozone and ethylene: A high-level quantum chemical and kinetic analysis of ozonolysis. *J. Phys. Chem. A* **2015**, *119*, 5524-5533.

- 36. Nakajima, M.; Yue, Q.; Endo, Y., Fourier-transform microwave spectroscopy of an alkyl substituted Criegee intermediate anti-CH₃CHOO. *J. Mol. Spectrosc.* **2015**, *310*, 109-112.
- 37. Levine, R. D., Molecular reaction dynamics. Cambridge University Press: New York, 2009.
- 38. Newland, M. J.; Rickard, A. R.; Alam, M. S.; Vereecken, L.; Munoz, A.; Rodenas, M.; Bloss, W. J., Kinetics of stabilised Criegee intermediates derived from alkene ozonolysis: reactions with SO₂, H₂O and decomposition under boundary layer conditions. *Phys. Chem. Chem. Phys.* **2015**, *17*, 4076-4088.
- 39. Kroll, J. H.; Sahay, S. R.; Anderson, J. G.; Demerjian, K. L.; Donahue, N. M., Mechanism of HOx formation in the gas-phase ozone-alkene reaction. 2. Prompt versus thermal dissociation of carbonyl oxides to form OH. *J. Phys. Chem. A* **2001**, *105*, 4446-4457.
- 40. Nguyen, T. L.; McCaslin, L.; McCarthy, M. C.; Stanton, J. F., Communication: Thermal unimolecular decomposition of syn-CH₃CHOO: A kinetic study. *J. Chem. Phys.* **2016**, *145*, 131102.
- 41. Long, B.; Bao, J. L.; Truhlar, D. G., Atmospheric chemistry of Criegee intermediates: Unimolecular reactions and reactions with water. *J. Am. Chem. Soc.* **2016**, *138*, 14409-14422.
- 42. Huang, H.-L.; Chao, W.; Lin, J. J.-M., Kinetics of a Criegee intermediate that would survive high humidity and may oxidize atmospheric SO₂. *Proc. Natl. Acad. Sci.* **2015**, *112*, 10857-10862.
- 43. Vereecken, L.; Novelli, A.; Taraborrelli, D., Unimolecular decay strongly limits the atmospheric impact of Criegee intermediates. *Phys. Chem. Chem. Phys.* **2017**, *19*, 31599-31612.
- 44. Vereecken, L.; Harder, H.; Novelli, A., The reaction of Criegee intermediates with NO, RO₂, and SO₂, and their fate in the atmosphere. *Phys. Chem. Chem. Phys.* **2012**, *14*, 14682-14695.
- 45. Percival, C. J.; Welz, O.; Eskola, A. J.; Savee, J. D.; Osborn, D. L.; Topping, D. O.; Lowe, D.; Utembe, S. R.; Bacak, A.; M c Figgans, G.; Cooke, M. C.; Xiao, P.; Archibald, A. T.; Jenkin, M. E.; Derwent, R. G.; Riipinen, I.; Mok, D. W. K.; Lee, E. P. F.; Dyke, J. M.; Taatjes, C. A.; Shallcross, D. E., Regional and global impacts of Criegee intermediates on atmospheric sulphuric acid concentrations and first steps of aerosol formation. *Faraday Discuss.* **2013**, *165*, 45-73.
- 46. Taatjes, C. A.; Shallcross, D. E.; Percival, C. J., Research frontiers in the chemistry of Criegee intermediates and tropospheric ozonolysis. *Phys. Chem. Chem. Phys.* **2014**, *16*, 1704-1718.
- 47. Chao, W.; Hsieh, J.-T.; Chang, C.-H.; Lin, J. J.-M., Direct kinetic measurement of the reaction of the simplest Criegee intermediate with water vapor. *Science* **2015**, *347*, 751-754.
- 48. Lewis, T. R.; Blitz, M. A.; Heard, D. E.; Seakins, P. W., Direct evidence for a substantive reaction between the Criegee intermediate, CH₂OO, and the water vapour dimer. *Phys. Chem. Chem. Phys.* **2015**, *17*, 4859-4863.
- 49. Berndt, T.; Kaethner, R.; Voigtlander, J.; Stratmann, F.; Pfeifle, M.; Reichle, P.; Sipila, M.; Kulmala, M.; Olzmann, M., Kinetics of the unimolecular reaction of CH₂OO and the bimolecular reactions with the water monomer, acetaldehyde and acetone under atmospheric conditions. *Phys. Chem. Chem. Phys.* **2015**, *17*, 19862-19873.
- 50. Anglada, J. M.; Bofill, J. M.; Olivella, S.; Solé, A., Unimolecular isomerizations and oxygen atom loss in formaldehyde and acetaldehyde carbonyl oxides. A theoretical investigation. *J. Am. Chem. Soc.* **1996**, *118*, 4636-4647.
- 51. Kuwata, K. T.; Hermes, M. R.; Carlson, M. J.; Zogg, C. K., Computational studies of the isomerization and hydration reactions of acetaldehyde oxide and methyl vinyl carbonyl oxide. *J. Phys. Chem. A* **2010**, *114*, 9192-9204.
- 52. Sheps, L.; Scully, A. M.; Au, K., UV absorption probing of the conformer-dependent reactivity of a Criegee intermediate CH₃CHOO. *Phys. Chem. Chem. Phys.* **2014**, *16*, 26701-26706.
- 53. Lin, L.-C.; Chao, W.; Chang, C.-H.; Takahashi, K.; Lin, J. J.-M., Temperature dependence of the reaction of anti-CH₃CHOO with water vapor. *Phys. Chem. Chem. Phys.* **2016**, *18*, 28189-28197.
- 54. Hakala, J. P.; Donahue, N. M., Pressure-dependent Criegee intermediate stabilization from alkene ozonolysis. *J. Phys. Chem. A* **2016**, *120*, 2173-2178.

- Taatjes, C. A.; Liu, F.; Rotavera, B.; Kumar, M.; Caravan, R.; Osborn, D. L.; Thompson, W. H.; Lester, M. I., Hydroxyacetone production from C3 Criegee intermediates. *J. Phys. Chem. A* **2017**, *121*, 16-23.
- 56. Kuwata, K. T.; Luu, L.; Weberg, A. B.; Huang, K.; Parsons, A. J.; Peebles, L. A.; Rackstraw, N. B.; Kim, M. J., Quantum chemical and statistical rate theory studies of the vinyl hydroperoxides formed in trans-2-butene and 2,3-dimethyl-2-butene ozonolysis. *J. Phys. Chem. A* **2018**, *122*, 2485–2502.
- 57. Pfeifle, M.; Ma, Y.-T.; Jasper, A. W.; Harding, L. B.; Hase, W. L.; Klippenstein, S. J. Nascent energy distribution of the Criegee intermediate CH₂OO from direct dynamics calculations of primary ozonide dissociation, *J. Chem. Phys.* **2018**, submitted.
- 58. Jasper, A. W.; Pelzer, K. M.; Miller, J. A.; Kamarchik, E.; Harding, L. B.; Klippenstein, S. J. Predictive a priori pressure-dependent kinetics. *Science* **2014**, *346*, 1212-1215.